Proceedings of the 9th U.S. National and 10th Canadian Conference on Earthquake Engineering
Compte Rendu de la 9ième Conférence Nationale Américaine et
10ième Conférence Canadienne de Génie Parasismique
July 25-29, 2010, Toronto, Ontario, Canada • Paper No 1280

EFFECTS OF POUNDING AND SKEWNESS ON SEISMIC RESPONSES OF MULTI-SPAN HIGHWAY BRIDGES USING FRAGILITY FUNCTION METHOD

Yili Huo[1] and Jian Zhang[2]

ABSTRACT

The seismic responses of multi-span highway bridges are affected by the geometry constraint (e.g. skewed alignment) and complex pounding behavior at expansion joints and end abutments, in addition to the nonlinear structural behavior and soil-structure interaction effects. In this paper, fragility functions describing seismic damage probabilities of highway bridges are derived and compared for bridges with various structural details, including the location of pounding gaps, deck alignment skew angle, and gap size. For bridges without pounding either due to their structural configurations or large gap sizes, the skewed geometry induces the coupled responses and subsequently improves seismic responses of bridges. For straight bridges, the pounding may cause significant local damage at expansion joints but its impact on bridge level damage is limited and practically neglectable. However, for skewed bridges, pounding results in observable increase of bridge damages and the skewness also aggravates the damage amplitude induced by pounding. The study clarifies the interactive role of skewness and pounding for the seismic responses of bridges and the findings can provide valuable guidance for future bridge design.

Introduction

The damage caused by pounding of adjacent bridge segments is one of the several most common damage forms experienced by highway bridges during past earthquakes (Chen and Duan 2003). It happens when excessive seismic displacement leads to the inadequate clearance (Priestly et al 1996), which results in pounding at gap locations (e.g. expansion joints or end abutments). The direct consequences of pounding range from minor damage at local level to major damage or collapse at global level (Chen and Duan 2003; Priestley et al 1991; Kawashima and Unjoh 1996 among others).

A number of studies have investigated the origin and outcomes of pounding for bridges

[1] Graduate Student Researcher, Dept. of Civil and Environmental Engineering, UCLA, Los Angeles, CA90095

[2] Assistant Professor, Dept. of Civil and Environmental Engineering, UCLA, Los Angeles, CA 90095

subject to seismic shakings. It has been well recognized that the pounding impact induces drastic and sudden spikes of the acceleration and contact force on the components involved in, which could generate severe local damages (Ruangrassamee and Kawashima 2001; Zhu et al. 2004). However, there are contradicting views on how pounding affects the global behavior of bridges. For example, Ruangrassamee and Kawashima (2001) illustrated that pounding results in additional damage in bridges, by showing that pounding increases the relative displacement spectrum. However, it was also shown that pounding reduces the bridge damages because the close of gaps stiffens the structure (McCabe and Hall 1989), disrupts the resonance buildup and dissipates energy (Priestley et al. 1996). Later, two other studies showed that pounding has little deteriorating effects on global damages, as it makes almost no change in displacement response despite the sharp rise of local acceleration and impact force (Kim and Shinozuka 2003; Ruangrassamee and Kawashima 2003). It appears that the pounding can be either beneficial or detrimental to bridge responses, depending on gap sizes, structural component properties and the earthquake ground motion characteristics (Jankowski 1998; Jankowski et al 2000; Zhu et al. 2004; Chouw and Hao 2008).

Recognizing the complexities involved with this problem, this study employs the fragility function method to study the effects of pounding and skewness on the seismic responses of multi-span RC bridges. Compared to the deterministic method, the fragility function method incorporates the variability and uncertainties of ground motion inputs and structural/foundation characteristics under a probabilistic framework. The damage probability of bridges in terms of engineering demand parameters (*EDP*s) exceeding certain limit states is derived. The selected *EDP* is directly and physically correlated to the bridge level damages hence can quantitatively monitor and describe the pounding effects. Furthermore, the study employs detailed three-dimensional bridge models for analyses, which realistically consider the soil-structure interaction effects, 3D structural responses and pounding at any location along the contact surface. Under this framework, the effects of pounding and skewness can be investigated systematically.

Modeling and Time History Analysis Procedure

Bridge Configurations

The selected bridge prototype is adapted from a design example by FHWA (FHWA 1996), which applies the AASHTO's seismic analysis and design requirements. Fig. 1 shows the geometry of the bridge and the reinforcement details of the pier column. The bridge represents a typical design in Western U.S.

Aiming to investigate the effects of pounding in bridges with different structural characteristics, three models, shown in Fig. 2(a-c) and named as models M1, M2 and M3, are built based on the prototype bridge. The model M1 is the original bridge design example, with continuous deck and monolithic abutments. The model M2 has seating type abutments, which induce gaps and therefore the possibility of pounding between the deck and the abutment wall at

each side. In model M3, an expansion joint is inserted at the center of the mid-span while the bridge has monolithic abutments. The deck and abutment can have either straight or skewed alignments for all three models as discussed below.

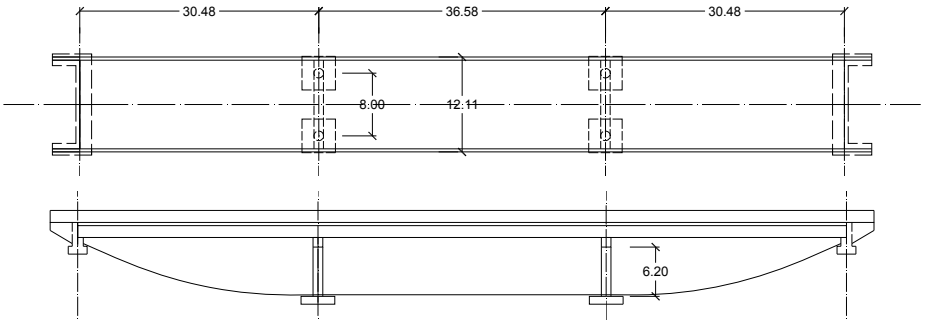

(a) Plan and elevation views

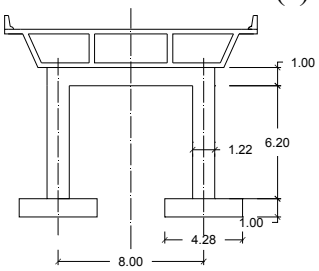

(b) Transverse cross-section of the bridge

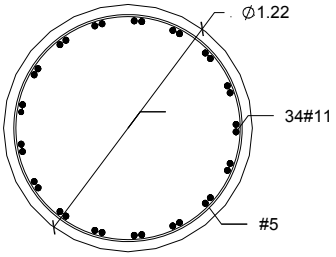

(c) Pier column cross section

Figure 1. The structural configurations of the prototype bridge (unit: m).

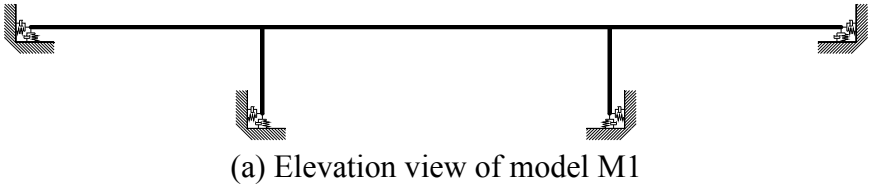

(a) Elevation view of model M1

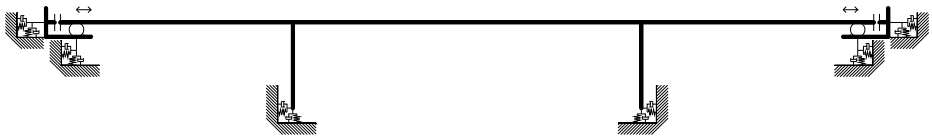

(b) Elevation view of model M2

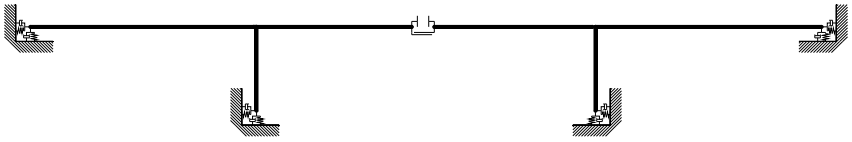

(c) Elevation view of model M3

Figure 2. The sketches of bridge models M1, M2 and M3.

Three-dimensional numerical models are built in software package OpenSees (http://opensees.berkeley.edu). The deck, bent beams, abutments are modeled with linear elastic

beam elements. To simulate the nonlinear behavior and capture the damage of pier columns, fiber section nonlinear beam elements, which are able to model the interaction between the axial force and bending moments, are employed. Distributed gap elements are utilized at the abutment connection in model M2 and at the expansion joint in model M3.

Ground Motions and Soil Structure Interaction Modeling

Fragility function method requires a large number of time history analyses to derive fragility functions; hence a great number of seismic ground motions are needed. This study selects 250 sets of ground motion records from the PEER strong motion database (http://peer.berkeley.edu/smcat). Each set of ground motion has two horizontal motion components and one vertical component. In each bridge model, abutment foundation consists of diagram wall and shallow foundation; pier columns are supported with shallow foundation. The numerical model utilizes equivalent linear springs and dashpots for simulating the soil-structure interaction (SSI) effects. For the embankment, the method developed by Zhang and Makris (2002) is applied to derive the modeling properties. For the pier shallow foundations, the modeling constants are calculated with the approach proposed by Gazetas (1991) and Mylonakis et al. (2006). As indicated by Chouw and Hao (2005), the spatially varied ground motion has pronounced effects on pounding phenomenon, and the mechanism of this spatial variation could be classified into two aspects, the wave propagation and the coherency loss. In this study, the wave propagation is taken into account with introducing the appropriate time lags of input motions along the wave propagating path. Regarding the site soil heterogeneity, the embankment material and geometry introduce the significant kinematic amplification on embankment motion and their effects are incorporated by method developed by Zhang and Makris (2002). Unlike the embankment fill, the kinematic effect of shallow foundations supporting the piers is considered as not significant. Therefore, the free-field ground motion is input at pier locations without further modification.

Nonlinear Time History Analysis Procedure

Different earthquake excitations, including previously discussed variance from both time lags and site amplification, are input at the locations of two abutment foundations and two pier shallow foundations. 3D ground motion is applied simultaneously with the larger horizontal component input in transverse direction. Nonlinear time history analyses are conducted and the displacements, pounding accelerations, pounding forces and pier column section curvatures throughout the entire bridge are monitored. Fig. 3 compares the time histories of deck acceleration, deck rotation, column drift and column section curvature responses between two M3 models with 4cm gap (with-pounding case) and sufficiently large gap (without-pounding case) respectively. Both models have a skewed angle of 30 degree. The ground motions recorded at 2516 Via Tejon PV station during the 1971 San Francisco Earthquake are scaled to peak ground acceleration of 0.8g and input as excitations.

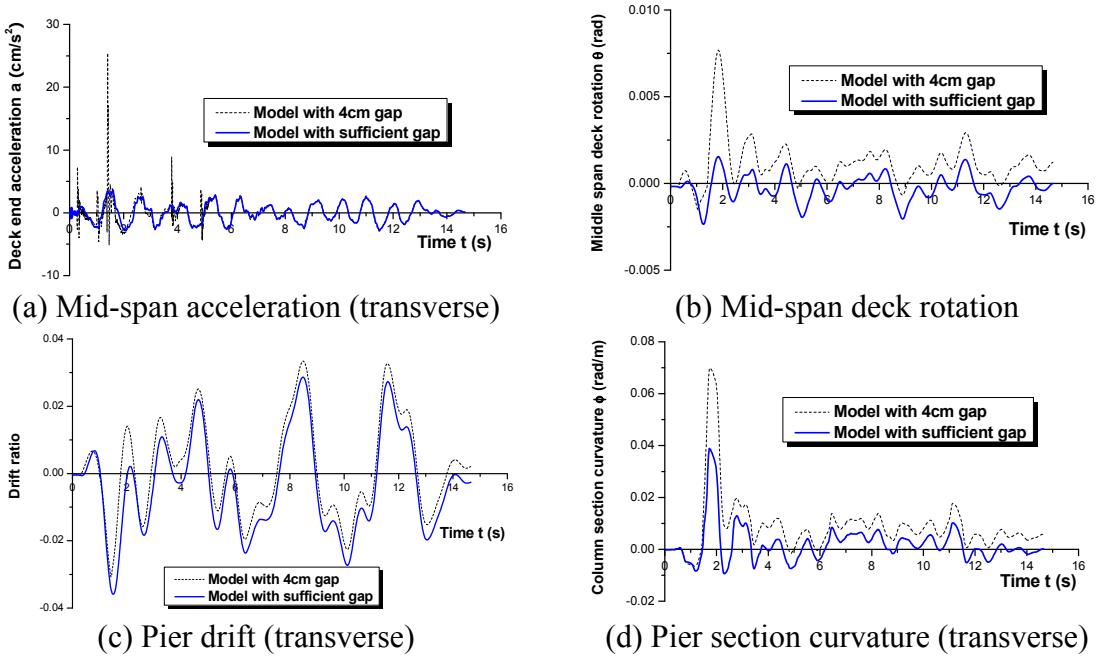

(a) Mid-span acceleration (transverse) (b) Mid-span deck rotation

(c) Pier drift (transverse) (d) Pier section curvature (transverse)

Figure 3. Time history responses of skewed M3 models (30°) under a sample earthquake

Fragility Analysis

Fragility function defines the conditional probability of attaining or exceeding a specified damage state for a given set of input intensity variables. A detailed discussion of the theory and application of the fragility function method can be found in Zhang and Huo (2009). In this study, peak ground acceleration (*PGA*) is utilized as the intensity measure (*IM*) of earthquake motions. The pier column section curvature is selected as damage index (*DI*). The yielding curvature κ_P is calculated and the limit state (*LS*) values suggested by Choi et al. (2004) are adopted for the four damage state (*DS*) levels defined in HAZUS (FEMA, 1999), as shown in Table 1.

Table 1. Limit state (*LS*) values for the four damage states (*DS*).

	Slight (*DS* =1)	Moderate (*DS*=2)	Extensive (*DS* =3)	Collapse (*DS* =4)
Physical sign (FEMA, 1999)	cracking and spalling	moderate cracking and spalling	degradation without collapse	failure leading to collapse
Section curvature κ (Choi et al, 2004)	$2\kappa_P > \kappa \geq \kappa_P$	$4\kappa_P > \kappa \geq 2\kappa_P$	$7\kappa_P > \kappa \geq 4\kappa_P$	$\kappa \geq 7\kappa_P$

This paper employs the incremental dynamic analysis (IDA) method for fragility analyses. The 250 sets of ground motions are scaled to 15 *PGA* levels, from 0.08g to 1.20g with 0.08g

increment. Nonlinear time history analyses are conducted at every *IM* level with the 250 motions. At any given *IM* level, the damage probability is calculated as the occurrence ratio of damage cases, i.e. the number of damage cases n_i for the damage state i over the number of total simulation cases N=250:

$$P\left[DI \geq LS \middle| IM\right] = \frac{n_i}{N} \qquad (i = 1 \text{ to } 4) \tag{1}$$

Typically, IDA fragility curves can be fitted with either normal cumulative distribution function:

$$P[DI \geq LS \mid IM] = \int_{-\infty}^{IM} \frac{1}{\sqrt{2\pi}\sigma_{IM}} \exp\left[-\frac{(im-\mu_{IM})^2}{2\sigma_{IM}^2}\right] d(im) \tag{2}$$

or lognormal cumulative distribution function:

$$P[DI \geq LS \middle| IM] = \int_{0}^{IM} \frac{1}{im\sqrt{2\pi}\xi_{IM}} \exp\left\{-\frac{\left[\ln(im)-\lambda_{IM}\right]^2}{2\xi_{IM}^2}\right\} d(im) \tag{3}$$

where μ_{IM} and σ_{IM} are mean value and standard deviation of *IM* to reach the specified damage state based on the normal distribution while λ_{IM} and ξ_{IM} are mean value and standard deviation of *IM* corresponding to the lognormal distribution.

With the above definitions and IDA approach, the fragility functions are developed for model M1 and shown in Fig. 4. Both normal and lognormal regressions are used to fit the raw fragility curves. The parameters for these regressions expressed by median and standard deviation are summarized in Table 2. The median value (μ in normal distribution or e^{λ} in lognormal distribution) represents the earthquake intensity (i.e. *PGA*) required to achieve the respective damage states. It is easy to find, by comparing the curves in Fig. 4 and data in Table 2, that bigger median values correspond to lower positioned fragility curves hence smaller damage probability. Therefore, the median values of the fragility curves can be used as a good indicator for characterizing the bridge vulnerability and will then be used to interpret the fragility results in the following parametric study.

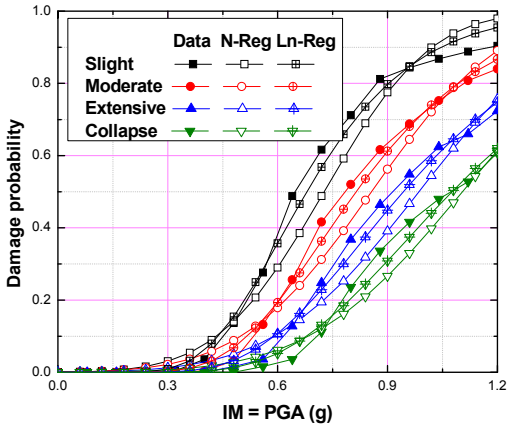

Figure 4. The IDA fragility curves for model M1 and the normal and lognormal regression.

Table 2. Median and standard deviation of normal and lognormal fragility curve regression

	DS=1		*DS*=3		*DS*=3		*DS*=4	
Normal μ_{IM} (g), σ_{IM}	0.73	0.23	0.86	0.28	0.99	0.31	1.11	0.33
Lognormal $e^{\lambda_{IM}}$ (g), ξ_{IM}	0.71	0.33	0.84	0.34	0.97	0.35	1.11	0.35

Effects of Skewed Geometry without Pounding

Prior to the study of pounding effect, the influence of skewed geometry is investigated first to clarify its effects. In bridge models M1, M2 and M3, the bent frames and abutments are rotated simultaneous with angles ranging from 15° to 60° , along with the vertical axis. The fragility functions of the model M1 with different alignment skew angles are derived and the median values corresponding to the assumed lognormal distribution are compared in Fig. 5. Since the higher median values are equivalent to smaller failure probability and hence the better performance, Fig. 5 demonstrates that increasing skew angles lead to better performance when pounding does not happen during the earthquake excitation. This result indicates that skewed geometry induces the coupled responses of bridges resulting in smaller column damages.

Similar analyses were also conducted with the models M2 and M3, in which the gap distance is assigned to a large value to prevent the pounding. For brevity, their fragility curves are not shown here. Nevertheless, similar beneficial effects of skewed geometry were also observed when pounding does not occur during the excitation.

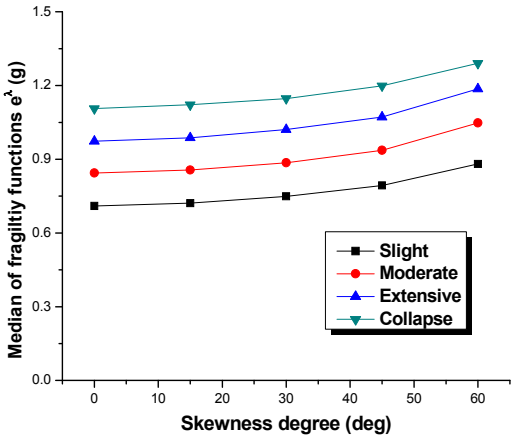

Figure 5. The median *IM*s of model M1 with various skewed angles.

Effects of Pounding for Straight Bridges

The gap distance in both models M2 and M3 is first set to be a typical value of 4cm and the bridge models with straight alignment are considered. In order to illustrate the pounding effects, the bridge models with 4cm gaps are compared with the identical models with gap

distance sufficiently large to prevent pounding from happening. The former models are noted as with-pounding cases while the latter ones are considered as without-pounding cases. A parameter *r* named as response ratio is defined as the ratio between the median values of fragility curves for with-pounding cases to that of the corresponding without-pounding cases:

$$r = \frac{e^{\lambda}(\text{with-pounding case, gap=4cm})}{e^{\lambda}(\text{without-pounding case, gap=}\infty)} \tag{4}$$

If the *r* value is larger than 1, it indicates that the with-pounding case requires larger median earthquake intensity (*PGA*) to reach the given damage states than the cases without-pounding. This is equivalent to a better performance indicating that the happenings of pounding during the earthquake actually protect the bridge piers from incurring larger damage probably due to the energy dissipation involved with pounding.

Fig. 6 shows the *r* values computed for models M2 and M3. For both models M2 and M3 at four damage states, the *r* values are larger than 1, which implies with-pounding cases for straight bridges yield better performance than the without-pounding cases. This observed beneficial effect could be explained by the mechanism that the happenings of pounding block further seismic displacements in bridges. The disrupted displacement increasing prevents more pier column deformation and thus reduces damages. Meanwhile, it is noticed that the values of response ratio *r* are actually very close to 1 although larger than 1. The with-pounding cases result in only less than 2% difference of the median earthquake intensity required for each damage state. Consequently, in spite of the slight benefit, the pounding effect in straight bridges can be treated as practically insignificant.

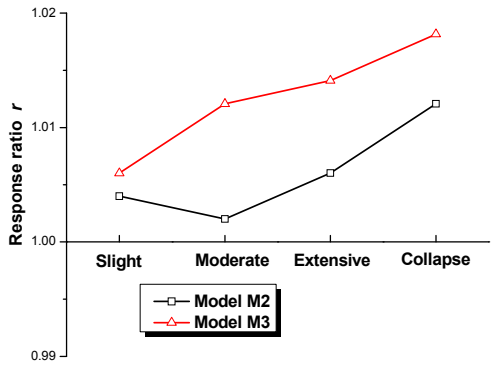

Figure 6. The response ratio *r* of models M2 and M3 with straight alignment.

Interactive Effects of Pounding and Skewed Geometry

In this section, the pounding effects are investigated in skewed-alignment bridges. Similar to the previous section, the parameter *r* recurs to reflect the pounding effects. Fig. 7 shows the *r* values of models M2 and M3 with skewness angle ranging from 0° to 60°. Contrast to the 0° (straight) cases where *r* is a slightly larger than 1, almost all skewed cases have *r* values smaller than 1. Therefore, the skewed bridges experience more damages due to pounding and

show worse performances for given earthquake intensity. The largest reduction reaches about 20%.

This detrimental effect of pounding can be explained by the increased pounding-induced rotation response in skewed bridges. The pounding causes more deck rotation for skewed bridges and thereby results in larger damages in pier columns, as can also be observed in the time history response shown in Fig. 3. Additionally, consistent with this conclusion, as shown in Fig. 7 larger skewness angle predictably intensifies the detrimental effects.

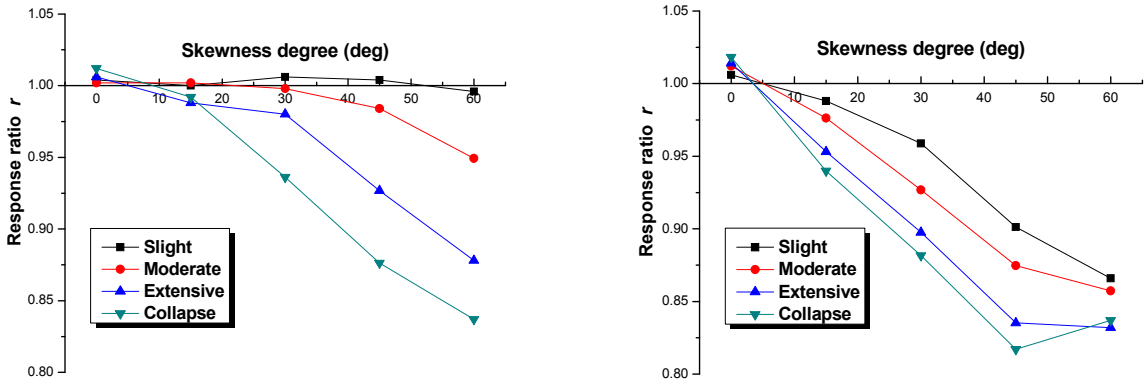

(a) Model M2 (b) Model M3

Figure 7. The response ratio *r* of models M2 and M3 with different skew angles.

Conclusions

In the paper, the fragility function method is adopted to study the effects of pounding and skewness in highway bridges. Three bridge models with different structural configurations in terms of location of gaps, gap size and skewed or straight geometry are analyzed with nonlinear three-dimensional time history analyses. By evaluating the median earthquake intensity required for reaching various damage states, the interactive effects of pounding and skewness are investigated. The study finds that: (a) The skewed geometry increases the coupled responses of bridges resulting in less damage of pier columns if no pounding is possible during the seismic excitation; (b) In straight bridges, the influence by pounding is small and almost practically neglectable; (c) In skewed bridges, the influence of pounding can be detrimental to bridge responses, opposite to that of straight bridges. By aggravating the rotation in bridges, pounding introduces larger seismic demand to pier columns. These findings can be used as basis for future bridge design, especially for cases with skewed geometry and pounding.

References

Chen, W-F. and L. Duan, 2003. *Bridge Engineering: Seismic Design*, CRC Press, Boca Raton, Florida.

Choi, E., R. DesRoches and B. Nielson, 2004. Seismic fragility of typical bridges in moderate seismic

zones, *Engineering Structures* 26, 187-199.

Chouw, N. and H. Hao, 2005. Study of SSI and non-uniform ground motion effect on pounding between bridge girders, *Soil Dynamics and Earthquake Engineering* 25, 717-728.

Chouw, N. and H. Hao, 2008. Response of bridge structures to spatially varying and site-amplified ground motion, *14th World Conference on Earthquake Engineering*, Beijing, China.

Federal Emergency Management Agency (FEMA), 1999. *Multi-Hazard Loss Estimation Methodology, Earthquake Model*. *HAZUS99 User's Manual*, Washington, DC.

Federal Highway Administration (FHWA), 1996. *Seismic Design of Bridges Design Example No.4: Three-Span Continous CIP Concrete Bridge*, Springfield, Virginia.

Gazetas, G., 1991. Formulas and charts for impedance of surface and embedded foundations, *Journal of Geotechnical Engineering ASCE* 117(9), 1363-1381.

Jankowski, R., K. Wilde and Y. Fujino, 1998. Pounding of superstructure segments in isolated elevated bridge during earthquakes, *Earthquakes Engineering and Structural Dynam*ics 27, 487-502.

Jankowski, R., K. Wilde and Y. Fujino, 2000. Reduction of pounding effects in elevated bridges during earthquakes, *Earthquake Engineering and Structural Dynamics* 29, 195-212.

Kawashima., K. and S. Unjoh, 1996. Impact of Hanshin/Awaji Earthquake on seismic design and seismic strengthening of highway bridges, *Structural Engineering and Earthquake Engineering JSCE* 13(2), 211-240.

Kim, S-H. and M. Shinozuka, 2003. Effects of seismically induced pounding at expansion joints of concrete bridges, *Journal of Engineering Mechanics* 129(11), 1225-1234.

McCabe, S. L., and W. J. Hall, 1989. Assessment of seismic structural damage, *Journal of Structural Engineering* 115(9), 2166–2183.

Mylonakis, G., S. Nikolaou and G. Gazetas, 2006. Footings under seismic loading: analysis and design issues with emphasis on bridge foundation, *Soil Dynamics and Earthquake Engineering* 26(9), 824-853.

Priestley, M. J. N., F. Seible and G. M. Calvi, 1996. *Seismic Design and Retrofit of Bridges*, Wiley, New York.

Priestley, M. J. N., J. P. Singh, T. L. Youd and K. M. Rollins, 1991. 6 Bridge. *Earthquake Spectral* 7(S2), 59-91.

Ruangrassamee, A. and K. Kawashima, 2001. Relative displacement response spectra with pounding effect, *Earthquake Engineering and Structural Dynamics* 30, 1511-1538.

Ruangrassamee, A. and K. Kawashima, 2003. Control of nonlinear bridge response with pounding effect by variable dampers, *Engineering Structures* 23, 593-606.

Zhang, J. and Y. Huo, 2009. Evaluating effectiveness and optimum design of isolation devices for highway bridges using fragility function method, *Engineering Structures* 31(8), 1648-1660.

Zhang, J. and N. Makris, 2002. Kinematic response functions and dynamic stiffnesses of bridge embankments, *Earthquake Engineering and Structural Dynamics* 31, 1933-1966.

Zhu, P., M. Abe and Y. Fujino, 2004. Evaluation of pounding countermeasures and serviceability of elevated bridges during seismic excitation using 3D modeling, *Earthquake Engineering and Structural Dynamics* 34, 591-609.